Non-Contact Instanteneous Heart Rate Monitoring using Microwave Doppler Sensor and Time-Frequency Domain Analysis

Daichi Matsunaga, Shintaro Izumi, Hiroshi Kawaguchi, and Masahiko Yoshimoto
Graduate School of System Informatics
Kobe University
Kobe, Japan
E-mail: matsunaga.daichi@cs28.cs.kobe-u.ac.jp

***Abstract*— This paper describes a non-contact heart rate monitoring system using a microwave Doppler sensor. It can achieve better usability than conventional heart rate sensors, which require direct skin contact. The objective of this work is to detect an instantaneous heart rate using this non-contact system. The instantaneous heart rate can contribute to prevent heart disasters and to detect mental stress state. However, the Doppler sensor system is very sensitive and it can be easily contaminated by a body motion artifact including breathing. To address this problem, we introduce time frequency analysis with short window length. The heart rate extraction performance with various parameters is evaluated using a measured Doppler sensor output with 4 subjects. The proposed method achieves 4.5-ms RMS error with 50-cm distance for heart rate extraction from 60 s duration data.**

Keywords-component; microwave Doppler, instantaneous heart rate, non-contact biosignal sensing, template matching

I. INTRODUCTION

The aging population in developed countries in recent years demands urgency of efforts to reduce health care costs. Prevention of lifestyle-related diseases including heart diseases such as myocardial infarction can be achieved through early detection and proper treatment. Preventing lifestyle-related diseases can be done by constantly monitoring physiological information. We specifically examined instantaneous heart rate information, which is particularly important for human beings. Analyses of the instantaneous heart rate can reveal a person's stress state and signs of heart disease.

To ascertain the heart rate, a 12-lead electrocardiograph, a Holter electrocardiograph, a photoelectric pulse wave meter [1–2], and a wearable electrocardiograph [3–5] are used. However, because all entail physical burdens, they present the problem that they are unsuitable for constant monitoring of physiological information. Therefore, we propose a non-contact and non-invasive instantaneous heart rate monitoring system using a microwave Doppler sensor.

Extending the time-frequency domain from the time domain data obtained from the Doppler sensor is effective [6]. This study evaluates the frequency analysis technique and its parameters for heart rate extraction from the Doppler sensor. A noise-tolerant instantaneous heart rate calculation algorithm is proposed as explained below.

This work was supported by JSPS KAKENHI Grant Number JP16H05868.

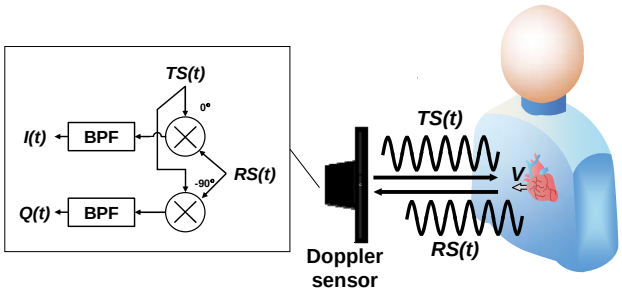

Fig. 1. Heart rate monitor using microwave Doppler sensor.

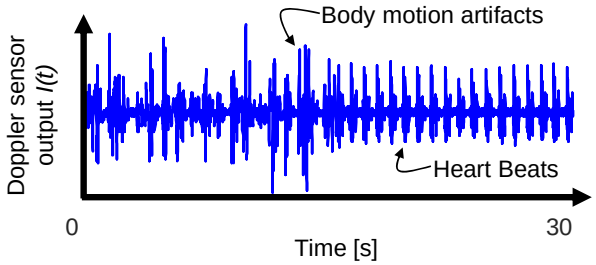

Fig. 2. Doppler wave *I(t)* including heart beat and body motion

II. MICROWAVE DOPPLER SENSOR

The Doppler sensor principles is clarified first. As presented in Fig. 1, a microwave Doppler sensor is used for this study. The output wave is a mixed wave incorporating the transmission wave (*TS*) from the Doppler sensor and a receiving wave (*RS*) reflected by the measurement object. The output is a Doppler wave $I(t)$ through a low pass filter. $I(t)$ is derived as shown below.

$$\mathrm{I(t)} = \frac{AA'}{2}\sin\left(\frac{2V}{\lambda}\times 2\pi t\right) \qquad (1)$$

In that equation, A, A', λ, and V respectively denote the transmitted wave amplitude, the received wave amplitude, the transmitted wave wavelength, and the target object velocity (m/s). By aiming this Doppler sensor at the chest of the person, a small vibration velocity that occurs on the body surface as a heartbeat is output as V. Then the instantaneous heart rate is found by calculating the distance between the regularly appearing V component. However, Doppler waves include the body motion velocity component W along with the heartbeat component. The output from the Doppler sensor at this time is expressed by the following equation.

$$\mathrm{I(t)} = \frac{AA_1'}{2}\sin\left(\frac{2W}{\lambda}\times 2\pi t\right) + \frac{AA_2'}{2}\sin\left(\frac{2(W+V)}{\lambda}\times 2\pi t\right) \quad (2)$$

If the body motion velocity component W is contained in the time domain, then heartbeat components are buried in noise and become invisible as depicted in Fig. 2. From equation (2), even if it includes body movement noise, the heart rate component V is included as frequency information. Therefore, by performing frequency analysis, heart rate component V and the body motion noise component W can be confirmed separately. In the following chapters, this report describes our examination of algorithms and the effects of parameters on frequency analysis.

III. Analysis Method

A. Time-frequency analysis using Most Entropy Method

Two approaches are used for frequency analysis. Non-parametric methods produce direct power spectral density (PSD) estimate from the input signals, similarly to a fast Fourier transform (FFT). A salient benefit of this approach is that the estimated PSD is accurate. However, it requires longer input data length to maintain the frequency resolution. To obtain the instantaneous heart rate, a spectrogram with fine time resolution is needed. Although it can be generated from short length data, the short input data length degrades the frequency resolution. Consequently, the input data length and frequency resolution in the non-parametric methods have a tradeoff relation. The PSDs from the short-term time frequency analysis must be used to acquire the instantaneous heart rate. Therefore, non-parametric methods are unsuitable.

In contrast, a parametric method models the input signal as an output of white noise passed through a particular linear system (filter). Therefore, this linear system can estimate the input signal PSD. Fig. 3 shows examples of 50-Hz sin wave PSDs estimated using the non-parametric (FFT) and the parametric (Burg's) method [7, 8]. To provide frequency analysis at a higher resolution from few data, we use the parametric method.

PSD estimation is represented as the following equation.

$$\boldsymbol{P}(f) = \frac{1}{F_s}\frac{\sigma^2}{\left|1-\sum_{i=1}^{M}\boldsymbol{a}_i e^{-j2\pi i f/F_s}\right|^2} \quad (3)$$

Here, F_s, σ^2, $\boldsymbol{a}$, and M respectively denote the sampling frequency, the expected value of the product of white noise of different times, the linear system parameter, and the order of the linear model. Bold letters denote column vectors. There are four kinds of estimation methods for this parameter; Yule-Walker AR, Burg, covariance and modified covariance method. For this study, we use Burg's method to estimate the linear system parameters. Burg's method can give higher resolution of the PSD estimate for short data than the Yule Walker AR method. Moreover, it always generates a stable model. Therefore, the measured Doppler sensor output can be separated in short windows to calculate the PSD.

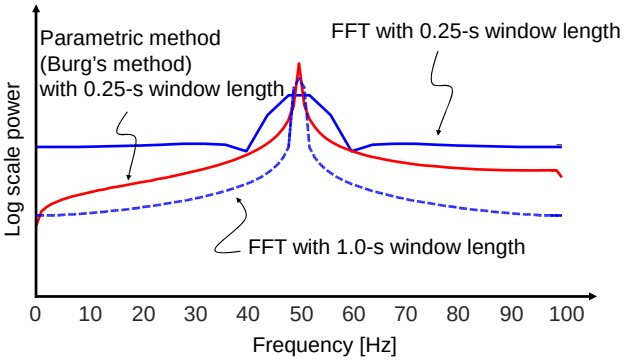

Fig. 3. Comparison of frequency resolution with 50-Hz sin wave input.

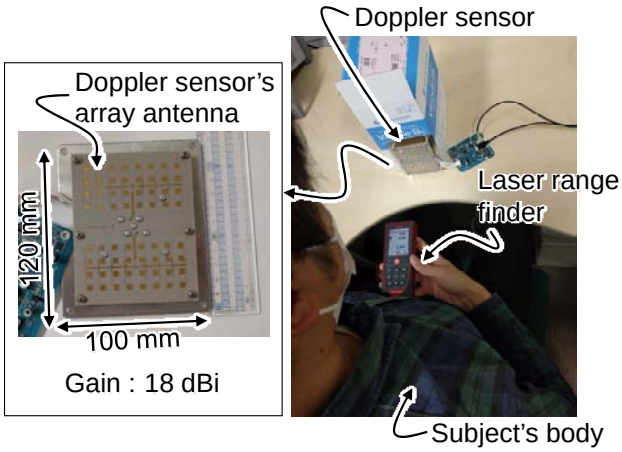

Fig. 4. Measurement environment.

B. Parameter determination for Burg's method

To obtain the accurate PSD with reasonable processing time, parameters of Burg's method should be optimized for this application. Both of the time resolution and the frequency resolution are affected by the window length, because it affects to the accuracy of the linear system parameter $\boldsymbol{a}$ in Eq. (3). The sampling frequency also affects to the accuracy because of the quantization error.

To determine the optimal order M, we use Akaike information criterion (AIC) [9] for order determination in this study. It prepares the candidates of a model that has different order, and determines the maximum log-likelihood. Then, as a correct model, it adopts a model having the largest maximum log-likelihood. However, if the order is larger, then a maximum log-likelihood also tends to increase. Therefore, in AIC, a model with large order has little likelihood of being chosen because of a penalty for large orders. AIC can be expressed as the following equation.

$$AIC = -2(\text{Maximum log} - \text{likelihood}) + 2(\text{degree of freedom of parameter}) \quad (4)$$

The degrees of freedom of the model parameters tend to be numerous in the higher order models. Therefore, the order with the smallest AIC is the optimal order. For this study, we use the following equation to calculate optimal order M.

$$AIC_i = \left(N - 2\sqrt{N}\right)(\log 2\pi + 1 + \log E) + 2(i+1) \quad (5)$$

$$M = \min_{1 \le i \le N - 2\sqrt{N}} AIC_i \quad (6)$$

In those equations, *N* and *E* respectively denote the length of input data and the residual variance of the model calculated using Burg's method. This AIC might vary according to the window width. As described in this paper, we compare the M of AIC with the maximum M of the window width.

Window length *N*, sampling frequency *Fs*, and model order *M* are evaluated in Section IV using measured data.

C. Template matching in a time-frequency domain

Our earlier report [10] proposed an autocorrelation and a template matching method used to extract the instantaneous heart rate from a noisy electrocardiogram. The peak of the coefficients is appearing regularly. We can calculate the instant heart rate from the peak coefficient intervals. In the previous work, template matching is used in one-dimension of the time domain. However, in the time-frequency domain analysis, it is difficult to decide the target frequency because the verbosity of the heart beat has different characteristics individually. It is affected by clothing, body type, and positional relation between the sensor and subjects. Therefore, this study expands this algorithm to two dimensions of the time-frequency domain. The calculation of the correlation coefficient *CC* between a template data and PSD at time *t* is expanded as following.

$$CC[t] = \sum_{i=-\frac{L_{win}}{2}}^{\frac{L_{win}}{2}-1} \sum_{f=1}^{F} TM[i][f] \cdot PSD[t+i][f] \quad (7)$$

Therein, L_{win}, *F*, *TM* and *PSD* respectively denote the window width, the upper limit of the frequency range, the generated template, and the PSD of Doppler sensor output. In this work, the window width and the frequency range were determined empirically as 0.5 s and 50 Hz.

IV. PERFORMANCE EVALUATION

The performance of the instantaneous heart rate extraction is evaluated using measured Doppler sensor output. The measurement environment is shown in Fig. 4. The heart rates for four men aged 22–23 were calculated. The duration of each measured data is 60 s for each subject.

We used a Doppler sensor (NJR4233D; New Japan Radio Co. Ltd.) for this experiment, which was conducted in our ordinary laboratory, not in a shielded room. Then, an ECG sensor is used as a reference sensor (Actiwave Cardio; CamNtech Ltd.), which obtain an accurate heart rate with 1-kHz sampling rate for validation.

We evaluated the effects of the parameters of window width *N*, sampling frequency *Fs*, order *M*, and the distance between the Doppler sensor and the subject. We calculated the root mean square (RMS) error between the reference sensor's instant heart rate and that obtained using the proposed method. The computing time was also evaluated using Matlab 2015b (The MathWorks Inc.) running on a personal computer (3.6 GHz core i7 processor by Intel Corp. and 8GByte working memory).

The RMS error was calculated as shown below.

$$\text{RMS error} = \sqrt{\frac{\sum_{t_n=1}^{N} (R_{IHR_{t_n}} - P_{IHR_{t_n}})^2}{N}} \quad (8)$$

In that equation, *N*, $R_{IHR_{t_n}}$ and $P_{IHR_{t_n}}$ respectively denote the number of data of the instant heart rate, the instant heart rate value obtained using the reference sensor, and the value obtained using the proposed method.

Figs. 5, 6, 7, 8 respectively show the evaluation results of the time frequency analysis, the sampling frequency, the window width, and the distance between the sensor and subjects. The RMS error and the processing time are affected by these parameters. We compared the RMS error performance with those reported in the literature [11] for another heart rate extraction system using an ultra-wide band Doppler sensor. Its RMS error was 5.1 ms, but its sample frequency and processing time are unknown.

Fig. 5 shows the example of power spectrogram of the Doppler wave analyzed by the proposed method with AIC. The heart beat signal can be found obviously, although it includes breathing.

Figs. 6 and 7 show that the processing time and the RMS error between the reference sensor output and calculated instantaneous heart rate. Then, the distance between the sensor and subjects is set to 50-cm.

In Fig. 6, the sampling frequency is swept from 100 Hz to 1 kHz. The window length is set to 100 ms in this evaluation. The conventional 1-dimensional template matching is conducted with three kinds of target frequency; 30, 40, and 50 Hz. The proposed 2-dimensional template matching always improves its RMS error compared with 1-dimention template matching. The AIC can reduce the processing time of the 2-dimensional template matching, it is about 29.7% at 800 Hz sampling frequency. When the sampling rate is higher than 200 Hz, there is only 0.63 ms RMS error difference regardless of AIC in the 2-dimensional template matching.

In Fig. 7, the window length is swept from 50 ms to 750 ms. The sampling rate is set to 1 kHz. Although the processing time is proportionally increased according to the window length, the RMS error has optimal point. A minimum RMS error is 4.5 ms in this evaluation with 100-ms window length.

Finally, we evaluated the effect of the distance between the sensor device and subjects as shown in Fig. 8. The distance is swept from 20 cm to 50 cm. The sampling rate and the window length is respectively set to 1 kHz and 100 ms. The 2-dimensional template matching with AIC shows better performance regardless of the distance. When the distance is set to 20 cm, the minimum RMS error is less than 3 ms.

V. CONCLUSION

To realize the non-contact instantaneous heart rate monitoring, this paper investigated about the time-frequency analysis method for the microwave Doppler sensor. To clarify the performance of the proposed system, the effect of the optimal order, the window width, the sampling rate, and the distance between the Doppler sensor and subjects was evaluated with measurement data. The proposed method using time-frequency analysis and 2-dimensional template matching achieves 4.50-ms RMS error with 50-cm distance.

As a matter left for examination in future work, body motion of the subject should be extracted from the same Doppler sensor and another filtering method. Stress and sleeping conditions can be examined by measuring both the instant heart rate and the breathing of the subject. Possible applications can be extended to car driver health monitoring, sleep state measurement, and early detection of heart disease.

REFERENCES

[1] L. Bor-Shyh, W. Chou, W. Hsing-Yu, H. Yan-Jun and P. Jeng-Shyang, "Development of Novel Non-Contact Electrodes for Mobile Electrocardiogram Monitoring System," *Proc. of IEEE Translational Engineering in Health and Medicine*, pp. 1–8, 2013.

[2] Y.M. Chi, S.R. Deiss and G. Cauwenberghs, "Non-contact Low Power EEG/ECG Electrode for High Density Wearable Biopotential Sensor Networks," *Sixth International Workshop on Wearable and Implantable Body Sensor Networks*, pp. 246–250, June 2009.

[3] K. Youngsung and C. Il-Yeon, "Wearable ECG Monitor: Evaluation and Experimental Analysis," *Proc. of International Conference on Information Science and Applications (ICISA)*, pp. 1–5, April 2011.

[4] C. Xianxiang, Xinyu Hu; R. Ren, Z. Bing, T. Xiao, X. Jiabai, F. Zhen, Q. Yangmin, L. Huaiyong and T. Lili, X. Shanhong, "Noninvasive Ambulatory Monitoring of the Electric and Mechanical Function of Heart with a Multifunction Wearable Sensor," *Proc. of IEEE COMPSACW*, pp. 662–667, July 2014.

[5] K. Hsein-Ping and J. Do-Un, "Wearable patch-type ECG using ubiquitous wireless sensor network for healthcare monitoring application," *Proc. of the Second International Conference on Interaction Sciences*, pp. 624–630, Nov. 2009.

[6] D. Matsunaga, S. Izumi, K. Okuno, H. Kawaguchi and M. Yoshimoto, "Non-contact and Noise Tolerant Heart Rate Monitoring using Microwave Doppler Sensor and Range Imagery," *Proc. of IEEE EMBC*, pp. 6118–6121, August 2015.

[7] K. Vos, "A Fast Implementation of Burg's Method," www.opus-codec.org/docs/vos_fastburg.pdf, August 2013, accessed 14.3.2016.

[8] N. Levinson, "The Wiener RMS error criterion in filter design and prediction." J. Math. Phys., v. 25, pp. 261278, 1947.

[9] T. Y. Kim, Y. H. Noh, D. U. Jeong, "On the use of the Akaike Information Criterion in AR spectral analysis of cardiovascular variability signals: a case report study," *Proc. of Computers in Cardiology*, Sep. 1993.

[10] Y. Nakai, S. Izumi, M. Nakano, K. Yamashita, T. Fujii, H. Kawaguchi and M. Yoshimoto, "Noise Tolerant QRS Detection using Template Matching with Short-Term Autocorrelation," *Proc. of IEEE EMBC*, pp. 6672–6675, August 2014

[11] T. Sakamoto, R. Imasaka, H. Taki, T. Sato, M. Yoshioka, K. Inoue, T. Fukuda, and H. Sakai, "Accurate heartbeat monitoring using ultra-wideband radar", *Proc. of IEICE Electronics Express*, Vol.12, No. 3, p.20141197, 2015

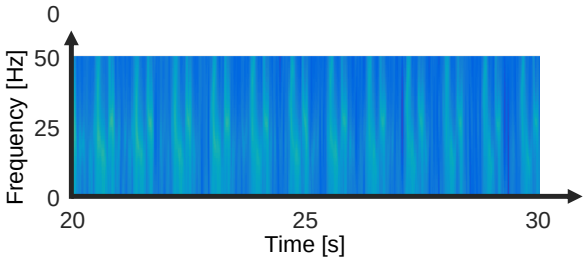

Fig. 5. Example of time-frequency analysis result with AIC order determination, 800-Hz Sampling rate, and 100-ms window width.

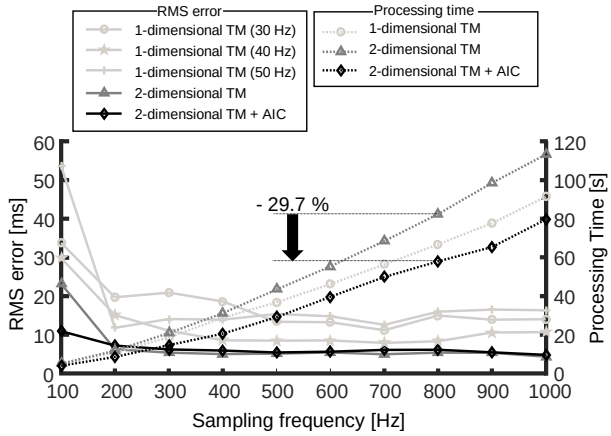

Fig. 6. Evaluation result of RMS error and processing time with 50-cm distance and 100-ms window width. Sampling rate is swept.

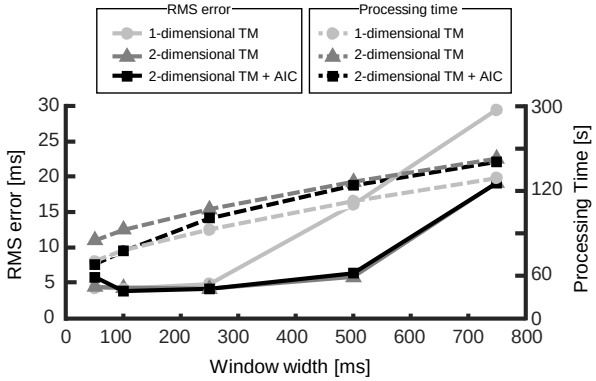

Fig. 7. Evaluation result of RMS error and processing time with 50-cm distance and 1-kHz sampling rate. Window width is swept.

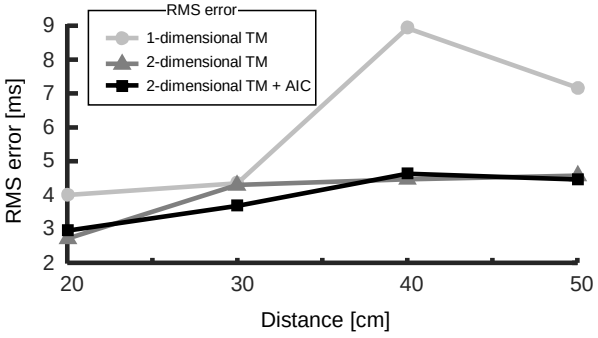

Fig. 8. Relation between RMS error and distance to subject with 1-kHz sampling rate and 100-ms window width.